PERGAMON

Organic Geochemistry 31 (2000) 1597–1610

Organic Geochemistry

www.elsevier.nl/locate/orggeochem

Composition of organic matter in subducted and unsubducted sediments off the Nicoya peninsula, Costa Rica (ODP Leg 170, Sites 1039 and 1040)

Rüdiger Lutz [a,*], Birgit Gieren [a], Andreas Lückge [b], Heinz Wilkes [c], Ralf Littke [a]

[a] *Institute of Geology and Geochemistry of Petroleum and Coal, Aachen University of Technology, Lochnerstr. 4-20, D-52056 Aachen, Germany*

[b] *Bundesanstalt für Geowissenschaften und Rohstoffe (BGR), Stilleweg 2, D-30655 Hannover, Germany*

[c] *Institute for Petroleum and Organic Geochemistry (ICG-4), Research Center Jülich GmbH, D-52425 Jülich, Germany*

Abstract

Investigation of sediment samples from Sites 1039 and 1040 (ODP Leg 170) drilled off the Nicoya peninsula (Costa Rica) by organic geochemical and organic petrological methods has revealed that subduction has only little influence on the composition of the sedimentary organic matter. Organic carbon contents reached 1.5% in the Pleistocene samples but Miocene and Pliocene sediments had an average organic carbon content of less than 0.5%. Organic carbon/sulfur ratios are generally below 2.8, reflecting an intense sulfate reduction in the uppermost sediments which was enhanced by sulfate supply both from sea water and deeper strata. Microscopical examinations indicate that the organic matter is mainly derived from marine sources. A small amount of terrigenous organic matter is, however, present as well according to *n*-alkane and fatty acid distributions. The alkenone unsaturation index $U^{k'}_{37}$ shows only a slight decrease during the Miocene and Pliocene, and stronger variations in the Pleistocene, probably indicating more stable sea surface temperatures during the Miocene and Pliocene. Variations in the Pleistocene can possibly be related to glacial/interglacial changes.

Keywords: Unstructured organic matter; Alkenones; SST; $U^{k'}_{37}$; Fatty acids; *n*-Alkanes; ODP; Costa Rica

1. Introduction

Subduction zones have a strong influence on earth, due to their widespread occurrence and the speed at which material is subducted. Material that enters the subduction zones is either accreted and leads to continental growth or is subducted into the mantle and influences the generation of magma. Subduction zones show a high seismicity and can therefore be easily identified (Frisch and Loeschke, 1993). The often high bioproductivity in near-shore areas (Berger et al., 1989) and high rates of clastic sedimentation — which includes the deposition of terrigenous and resedimented organic material — means that there is a high potential for organic matter to be subducted. It is, therefore, important to investigate the emergence and development of subduction zones and the fate of organic matter within these zones.

The subduction zone off Costa Rica has been the focus of various studies prior to ODP Leg 170. During Leg 84, Site 565 was drilled into the midslope of the Costa Rica Margin to a depth of 328 mbsf and gas hydrates were recovered (von Huene and Aubouin, 1985). Other investigations included studies of seismic data of the subduction zone (Shipley et al., 1992; Hinz et al., 1996) and heatflow measurements (Langseth and Silver, 1996). With Leg 170 and the sites drilled during the cruise, an exceptional opportunity existed to study the influences of subduction. We studied the organic matter with different petrological and organic geochemical

* Corresponding author. Fax: +49-241-8888152.
E-mail address: lutz@lek.rwth-aachen.de (R. Lutz).

0146-6380/00/$ - see front matter
PII: S0146-6380(00)00089-9

techniques to reveal the nature of the organic matter and the influences of diagenesis on the subducted and unsubducted sediments at an early diagenetic stage. Results of this study will furnish input parameters for an additional numerical modelling of thermal hydrocarbon generation off Costa Rica. Total organic carbon (TOC), total carbon (TC) and sulfur (S) were measured to determine the bulk composition of the sediments. To reveal the nature of the organic matter, i.e. terrigenous vs. marine organic matter, microscopic studies and Rock-Eval pyrolysis were performed and *n*-alkane and fatty acid distributions were studied. Rock-Eval data, *n*-alkane and fatty acid distributions and microscopic constituents are influenced by early diagenetic processes. Concentration of sulfate in porewaters was used to show the extent of sulfate reduction as a major early diagenetic process in organic matter destruction/alteration. Alkenone concentrations, palaeoproductivities and accumulation rates were determined/calculated to shed light on the palaeoenvironment.

2. Geological setting

The studies on organic matter presented in this paper were carried out on samples from two ODP sites drilled off Costa Rica (Fig. 1). Site 1039 is situated about 1.5 km off the Middle America Trench on the seaward side and serves as a reference site, because the sedimentary succession of the Cocos plate is undeformed there. The Cocos plate is subducted at the Middle America Trench with a velocity of about 85 mm/a off Costa Rica (Kimura et al., 1997). At Site 1039 the sediments can be divided into three units. Unit U1 consists of diatomaceous ooze with ash and sand layers. Unit U2 consists of silty clay with ash layers and U3 is built of siliceous

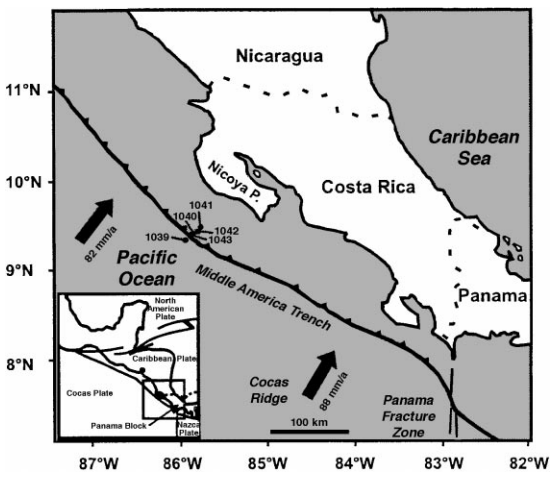

Fig. 1. Location of the sites drilled during ODP Leg 170.

nannofossil ooze. Site 1040 is located about 1.5 km off the subduction zone on the landward side. At this site, wells were drilled through the accretionary prism and decollement into the subducted sedimentary succession. At Site 1040 the sediments can be divided into four units. Unit P1 comprises the sediments of the accretionary prism which consist of silty clay with debris flows. In the accretionary prism an age-depth correlation could not be made, because the microfossils are reworked and paleomagnetic data could not be assigned to the magnetic polarity time scale (Kimura et al., 1997). Below the decollement the same units U1 to U3 as at Site 1039 were found. These units are more compacted at Site 1040, reduced in thickness and more lithified but lithologies are very similar and sediments represent the same time span — from middle Miocene to late Pleistocene. They also contain microfossil assemblages which are very similar to those at Site 1039 (Kimura et al., 1997).

3. Samples

In this study, 36 sediment samples from Site 1039 and 35 sediment samples from Site 1040 were investigated. Total organic carbon (TOC), total carbon (TC) and sulfur (S) measurements were carried out on whole rock samples. Kerogen concentrates for further studies were prepared from five samples from Site 1039 and six samples from Site 1040 with TOC values $>0.5\%$. On the kerogen concentrates, TOC-, S- and Fe contents were determined and Rock-Eval pyrolysis and microscopic studies were performed. Thirteen samples from Site 1039 and 9 samples from Site 1040 were selected for characterization of the extractable organic matter.

4. Experimental

Our investigations used freeze dried and pulverized samples. TC, TOC and S contents were measured with a LECO CS-225 (Carbon-Sulfur-Determinator). Carbonate-carbon contents were calculated as $CaCO_3$-equivalents according to the equation:

$$CaCO_3\ (\text{wt.}\%) = (TC - TOC)\cdot\frac{100.9}{12.01} \quad (1)$$

Rock-Eval pyrolysis was performed with a DELSI Rock-Eval-II instrument (Espitalié et al., 1985). Hydrogen index (HI) values (mg hydrocarbon-equivalents per gram of TOC), Oxygen index (OI) values (mg CO_2 per gram of TOC) and T_{max} values (temperatures of maximum pyrolysis yield) were determined on whole rock samples and kerogen concentrates. Kerogen concentrates were obtained by treatment with hydrochloric

acid (HCl) and hydrofluoric acid (HF) to dissolve carbonates and silicates (Durand and Nicaise, 1980). Fe contents were determined with an atomic absorption spectrometer, Perkin Elmer, Type 3030.

Microscopic studies were performed on polished blocks of sediments and kerogen concentrates in white reflected light and in fluorescence induced by ultra-violet/violet light (Taylor et al., 1998). Blocks were made by embedding either sediments or kerogen concentrates in resin (Scandiplex).

Bulk sediment accumulation rates were calculated using the equation (Stein, 1991):

$$AR_{\mathrm{SED}} = SR * \left(\rho_{\mathrm{wet}} - 1.026PO * 10^{-2}\right) \quad (2)$$

AR_{SED} Bulk sediment accumulation rate ($g * cm^{-2}\ a^{-1}$)
SR Sedimentation rate ($cm * a^{-1}$)
ρ_{wet} Wet bulk density ($g * cm^{-3}$)
PO Porosity (%)

Accumulation rates for single components, e. g. organic matter, were calculated by multiplication of AR_{SED} with the content of the component in wt.% and division by 100.

Paleoproductivity at Sites 1039 and 1040 was calculated with the empirically derived equation for normal marine sediments (i.e. sediments deposited under oxic marine conditions) after Stein (1986):

$$PP = 5.31(\mathrm{C}_{\mathrm{marine}}(\rho_{\mathrm{wet}} - 1.026PO{*}10^{-2}))^{0.71} * SR^{0.07} * D_{\mathrm{Water}}^{0.45} \quad (3)$$

PP Primary productivity ($g\ C\ m^{-2}\ a^{-1}$)
$\mathrm{C}_{\mathrm{marine}}$ Marine organic carbon (wt.%)
SR Sedimentation rate ($cm\ ka^{-1}$)
D_{Water} Water depth (m)

Physical properties and sedimentation rates for calculations were taken from the Initial Reports of ODP Leg 170 (Kimura et al., 1997). Stein (1991) discussed the pitfalls in palaeoproductivity calculation.

For lipid analysis, sediment samples were extracted using a modified flow-blending method (Radke et al., 1978) with dichloromethane-methanol (99:1). Extracts were separated into acids, bases, high-, medium- and low-polarity nitrogen-, sulfur- and oxygen-containing (NSO) compounds, and aromatic and aliphatic hydrocarbons by liquid chromatography according to the method of Willsch et al. (1997). Aliphatic hydrocarbons, fatty acids after methylation with diazomethane, and low-polarity NSO compounds which include the long-chain alkenones were analyzed by gas chromatography (GC). GC of aliphatic hydrocarbons and long-chain alkenones was conducted on a Hewlett-Packard 5890 Series II instrument equipped with an on-column-injector, flame ionization detector and a fused silica capillary column (HP Ultra I) of 50 m length, 0.2 mm inner diameter and 0.33 μm film thickness. Hydrogen was used as carrier gas, and the oven temperature was programmed from 90°C (hold time, 5 min) to 310°C at a rate of 4°C/min (aliphatic hydrocarbons) or 3°C/min (long-chain alkenones). GC of fatty acid methyl esters was performed on a Hewlett-Packard 5890 Series II instrument equipped with a cold-injection system (KAS; −50–300°C, 10°C/s, 3 min hold time), flame ionization detector and a fused silica capillary column (SGE BPX5) of 50 m length, 0.1 mm inner diameter and 0.25 μm film thickness. Helium was used as carrier gas, and the oven temperature was programmed from 120°C (hold time 2 min) to 320°C at a rate of 3°C/min. 5α-Androstane, cholesteryl hexanoate and perdeuteroicosanoic acid methyl ester were used as internal standards for the quantification of aliphatic hydrocarbons, long-chain alkenones and fatty acid methyl esters, respectively.

The carbon preference index for hydrocarbons (CPI_{HC}) was calculated according to the equation:

$$CPI_{\mathrm{HC}} = \frac{(\mathrm{C}_{21} + \mathrm{C}_{23} + \mathrm{C}_{25})}{(\mathrm{C}_{29} + \mathrm{C}_{31} + \mathrm{C}_{33})} \quad (4)$$

Values for even-over-odd predominance (EOP) of n-alkanes were calculated according to the equation:

$$EOP = \frac{2 * (\mathrm{C}_{18} + \mathrm{C}_{20} + \mathrm{C}_{22})}{(\mathrm{C}_{17} + 2 * \mathrm{C}_{19} + 2 * \mathrm{C}_{21} + \mathrm{C}_{23})} \quad (5)$$

The carbon preference index for fatty acids (CPI_{FA}) was calculated according to the following equation:

$$CPI_{\mathrm{FA}} = \frac{(\mathrm{C}_{14} + \mathrm{C}_{16} + \mathrm{C}_{18})}{(\mathrm{C}_{14} + \mathrm{C}_{16} + \mathrm{C}_{18} + \mathrm{C}_{24} + \mathrm{C}_{26} + \mathrm{C}_{28})} \quad (6)$$

The alkenone unsaturation index $U_{37}^{k'}$ was calculated according to Brassell et al. (1986):

$$U_{37}^{k'} = \frac{[\mathrm{C}_{37:2}]}{([\mathrm{C}_{37:2}] + [\mathrm{C}_{37:3}])} \quad (7)$$

$\mathrm{C}_{37:2}$ 15*E*, 22*E*-Heptatriacontadien-2-one
$\mathrm{C}_{37:3}$ 8*E*,15*E*,22*E*-Heptatriacontatrien-2-one

Paleo sea surface temperatures were calculated after Müller et al. (1998):

$$U_{37}^{k'} = 0.033 * T + 0.069 \quad (8)$$

T Temperature (°C)

Sulfate concentration data of Sites 1039 and 1040 was taken from the Proceedings of the Ocean Drilling Program Vol. 170 (Kimura et al., 1997).

5. Results and discussion

5.1. Organic and inorganic carbon contents

At Site 1039 organic carbon contents are highly variable (Fig. 2). The values range from a maximum of 1.6% in a near surface sample in unit U1 to a minimum of 0.1% in unit U3 (below 225 mbsf). The average organic carbon content in unit U1 is ~1%. In unit U2 the value decreases to $<0.5\%$ and drops to $<0.2\%$ in unit U3. Thus, TOC contents clearly decrease from top to bottom of the core. The Miocene to early Pliocene unit U3 shows typical TOC values for open marine environments with low organic productivity (Stein, 1991) and can be assigned to a pelagic depositional environment. The Pliocene to Pleistocene units U1 and U2 resemble typical hemipelagic environments (Kimura et al., 1997).

At Site 1040 TOC contents vary between 0.1 and 1.3% (Fig. 3). In unit P1 the average TOC content is 0.9% and shows only small variations with depth. At the top of unit U1 the organic carbon content is even higher; a maximum value of 1.3% was determined for a sample from this unit (391.34 mbsf). Below this unit the TOC contents decrease nearly continuously to an average value of 0.1% in unit U3. Units U1 to U3 at Site 1040 show the same depth trend for TOC values as at Site 1039, i.e. a decrease in TOC contents from top to bottom. In contrast there is no such tendency in unit P1, because of the heterogeneous composition and the mixture of the sediments in the accretionary wedge.

The content of inorganic carbon, expressed here as $CaCO_3$-equivalents, varies from 0.7 to 79.8% at Site 1039 (Fig. 2). $CaCO_3$ contents in unit U1 are less than 5%, with few exceptions. In unit U2 the contents are generally less than 4% and only reach 7.6% at the transition to unit U3. Sediments of unit U3 show the highest $CaCO_3$ values. The average $CaCO_3$ content is 31%. Unit U3 is a highly calcareous sequence, whereas units U1 and U2 can be summarized as carbonate-lean sediments. These findings indicate a change in the depositional environment, from pelagic to hemipelagic sedimentation.

Carbonate contents in sediment samples at Site 1040 vary from 1.5 to 82.3% (Fig. 3). Unit U3 has an average carbonate content $>50\%$. Just below the transition to unit U2, the values increase and reach a maximum of 82.3%. In units U1 and U2, $CaCO_3$ contents are significantly lower than 5%. Above the decollement in sediments of unit P1, $CaCO_3$ contents are less than 6%. At both sites a drastic increase in $CaCO_3$ contents is recorded in unit U3 (Figs. 2 and 3). At Site 1039 this increase starts at a depth of 180 mbsf and at Site 1040 it is recorded for a depth of 120 m below the decollement. Considering the different reduction of sediment thickness for both sites the two profiles are well correlated.

Using the organic carbon and carbonate content data, accumulation rates were calculated (Table 1). Accumulation rates are a tool to compare differently compacted sediments, and dilution effects do not influence single components (e. g. TOC, $CaCO_3$; Stein, 1991). Accumulation rates for inorganic carbon at both sites are >20 g $CaCO_3$ m^{-2} a^{-1} for the middle Miocene. These values decreased strongly towards the Late Miocene and Pliocene and increased slightly again in the Pleistocene (Table 1). Accumulation rates for organic carbon were constantly low (<0.1 g C m^{-2} a^{-1}) during the Middle Miocene to Pliocene. In the Pleistocene accumulation

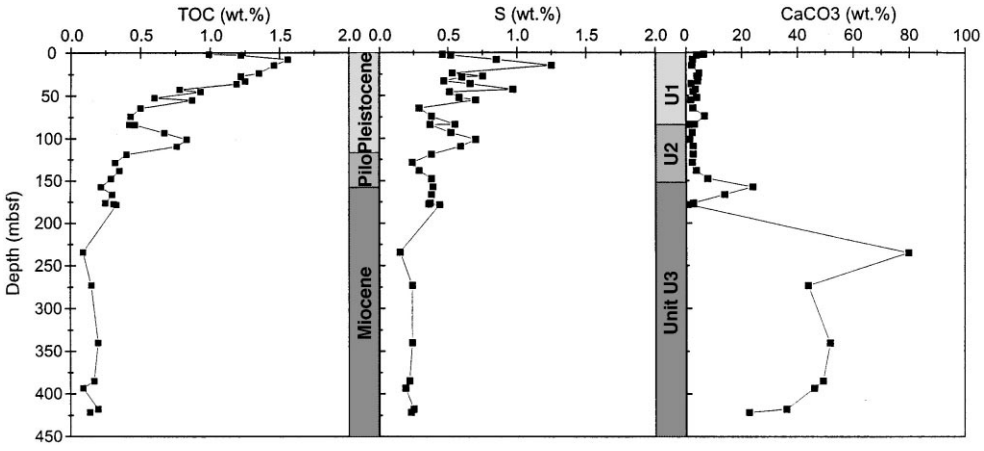

Fig. 2. Depth profiles of organic carbon, sulfur and carbonate contents for Site 1039.

rates for organic carbon increased to 0.3 g C m^{-2} a^{-1} at Site 1039 and 0.6 g C m^{-2} a^{-1} at Site 1040. The significantly higher accumulation rates in the Pleistocene do not correspond to a distal open marine environment, but are more typical of a near-shore environment. Values in the same range were calculated, among others, for ODP Sites 955A and 956A off Gran Canaria (Littke et al., 1998).

The calculated paleoproductivity values increase with decreasing age (Table 1). The enhancement of paleoproductivity and accumulation rates can be related to the drift of the Cocos plate to a near-shore position. Comparison of the paleoproductivity and recent productivity of the ocean (Koblents-Mishke et al., 1970) shows good correspondence, i.e. the calculated values for today are in the same range as those measured for today. It has to be taken into account, that calculations are estimations rather than exact calculations, because several important parameters are neglected, e.g. different source organisms (Littke et al., 1997a). Furthermore, the early diagenetic alteration of organic matter can significantly reduce organic carbon percentages; this effect can be stronger than that of palaeoproductivity differences (Canfield, 1989; Pedersen & Calvert, 1990; Calvert & Pedersen, 1992). One example are sediments offshore Pakistan, where a thick oxygen minimum layer exists and where more than 50% of the sedimentary organic matter was consumed by bacterial sulfate reduction within the uppermost two meters of the sediments (Littke et al., 1997b). Considering the accumulation rates for organic and inorganic carbon, the paleoproductivity values and the organic carbon contents in the Middle and Late Miocene it can be concluded that the organic carbon was diluted by enhanced accumulation of carbonate during the Middle Miocene. This is supported by calculations of organic carbon (TOC*) in a (hypothetic) carbonate-free sediment. In the carbonate-rich Miocene sequence, TOC* values vary between about 0.2 and 0.8%, with some exceptions. The average value is 0.5%. This value is only slightly smaller

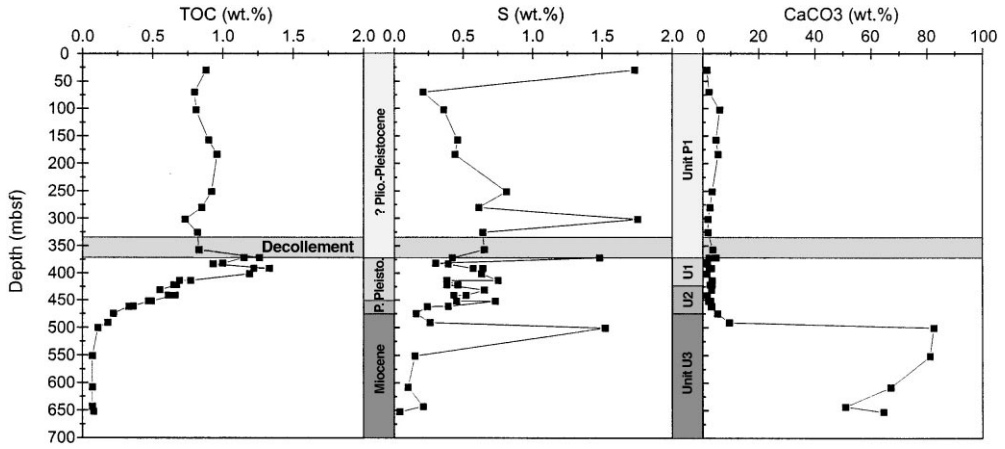

Fig. 3. Depth profiles of organic carbon, sulfur and carbonate contents for Site 1040.

Table 1
Averages of organic carbon and carbonate concentrations (weight percent), accumulation rates and surface water paleo-productivities calculated for various stratigraphic intervals of Sites 1039 and 1040. The paleo-productivities were calculated according to Stein (1991), and are not corrected for early diagenetic organic carbon loss

	TOC (%)	$CaCO_3$ (%)	AR_{TOC} (g C m^{-2} a^{-1})	AR_{CaCO3} (g $CaCO_3$ m^{-2} a^{-1})	PP (g C m^{-2} a^{-1})
Site 1039					
Pleistocene	0.92	3.11	0.3	1.0	135
Pliocene	0.32	4.48	0.01	0.2	67
1. Miocene	0.28	8.67	0.02	0.4	62
m. Miocene	0.15	47.03	0.07	20.6	53
Site 1040					
Pleistocene	0.92	2.39	0.6	1.4	227
l. Mio-Pliocene	0.31	15.43	0.02	1.0	88
m. Miocene	0.07	65.79	0.02	21.7	34

than in the overlying U2 unit (average 0.6%), but clearly smaller than in U1 (average 1.1%). Differences between the two sites are minor, perhaps with the exception of carbonate contents in the Miocene to Pliocene sequence. The only small variability is expected, since the depositional sites are close together (Fig. 1). Nevertheless, differences in sedimentation rates are reported by Kimura et al. (1997), probably due to the stratigraphic resolution.

5.2. Sulfur contents

Sulfur contents in the sediment samples from Site 1039 vary between 1.3% in unit U1 and 0.2% in unit U3 (Fig. 2). The sulfur contents decrease with increasing depth such as TOC values, but show larger variations.

The sulfur contents at Site 1040 range from a minimum of 0.04% in unit U3 to a maximum of 1.8% in unit P1. In contrast to the TOC values the sulfur values vary significantly in unit P1 (0.2–1.8%). This could be related to an allochthonous input of pyrite at the slope by turbidites or debris flows. At Site 1040 sulfur contents rise immediately below the decollement to 1.5% in unit U1. In unit U2, sulfur contents decrease nearly constantly from 0.7 to 0.2% and in U3 sulfur contents are less than 0.3%, with one exceptional value of 1.5%. The subducted sediments at Site 1040 show the same tendency of sulfur content decrease with increasing depth as those at Site 1039, but with greater scatter.

The empirically derived ratio of organic carbon to sulfur for sediments deposited under oxic conditions (normal-marine) is about 2.8 (Berner, 1983; Berner and Raiswell, 1983). Most samples from Sites 1039 and 1040 plot above the trendline representing the C/S ratio of 2.8 (Fig. 4). According to criteria developed by Berner and Raiswell (1983) this indicates a highly effective sulfate reduction system and the likely presence of anoxic conditions in the water column or in bottom waters. However, high sulfate concentrations in porewaters below the sediment/water interface contradict this idea, at least for the present time (Kimura et al., 1997). The sulfate concentrations at Site 1039 decrease significantly to a depth of 24 mbsf due to sulfate reduction (Fig. 5). Below 24 mbsf sulfate concentrations rise continuously. The minimum concentration of 13.2 mmol/l indicates that sulfate availability was not the limiting factor for sulfate reduction. Sulfate was transported from seawater and deeper sediments — which are lean in organic matter and, therefore, sulfate rich — into the zone of intensive sulfate reduction.

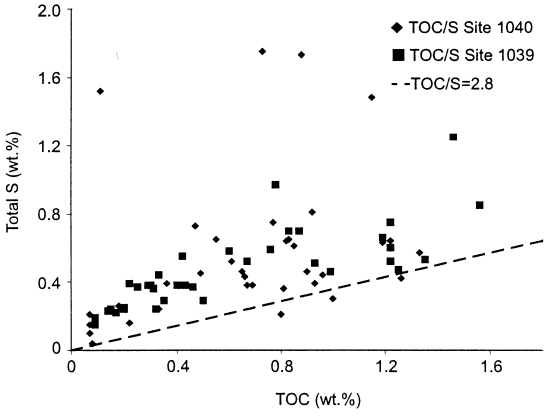

Fig. 4. Total sulfur and organic carbon for samples from Sites 1039 and 1040.

Sulfate concentrations in porewaters at Site 1040 show a steep concentration gradient and are below the detection limit at a depth of 30 mbsf (Fig. 5). This strong decrease was caused by sulfate reduction. In contrast to Site 1039, sulfate became exhausted here, thus limiting further sulfate reduction. The complete sulfate consumption may be related to high sedimentation rates (>100–150 m/Ma; Kimura et al., 1997) and thus, limited transport of sulfate from seawater into the rapidly subsiding sediments. In unit P1 no sulfate can be detected below 30 mbsf. Below the decollement at a depth of 410.18 mbsf, sulfate concentrations start to rise continuously from 2.5 to 28.0 mmol/l at a depth of 652.88 mbsf. The value of 28.0 mmol/l is nearly equal to the typical value of 28.25 mmol/l for seawater with a salinity of 35‰ (Chester, 1990).

High sulfate concentrations at the top of unit P1 indicate that anoxic conditions did not exist in the oceanic bottom water. Anoxic conditions at the top of the subducted sediments recently exist, because sulfate transport from seawater was stopped by underthrusting and the remaining sulfate was consumed by microbial activity (Kimura et al., 1997).

Most of the sulfur (70–90%) in the studied kerogen concentrates is fixed as pyrite. This can be inferred from the ratio of sulfur to iron (S/Fe = 1.15 in pyrite). Ten to thirty percent of the sulfur is fixed either in inorganic sulfur-containing compounds, which were not destroyed by hydrochloric and hydrofluoric acid treatment, or in the organic matter (Sinninghe Damsté et al., 1989). Some sulfur fixed in inorganic sulfur-containing compounds must have been lost during kerogen concentration as indicated by higher S/TOC ratios in sediments compared to kerogen concentrates. Type II kerogen, in particular, may contain medium to high sulfur amounts (Tissot and Welte, 1984).

5.3. Quality of organic matter

HI and OI values are presented in Fig. 6. HI values for whole rock samples from Site 1039 vary between 13 and 491 mg HC/g TOC. HI values of kerogen concentrates range from 159 to 311 mg HC/g TOC. OI values of whole rock samples are very high, between 120

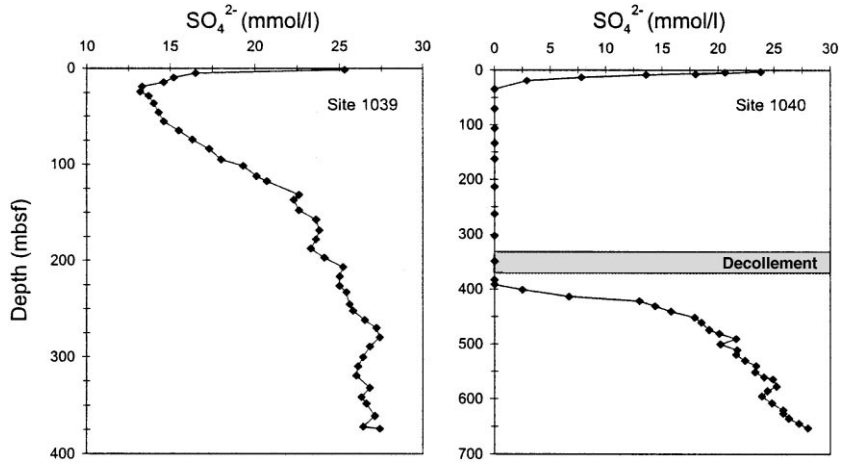

Fig. 5. Concentration depth profiles of sulfate in porewaters of samples from Site 1039 and 1040 (Kimura et al., 1997).

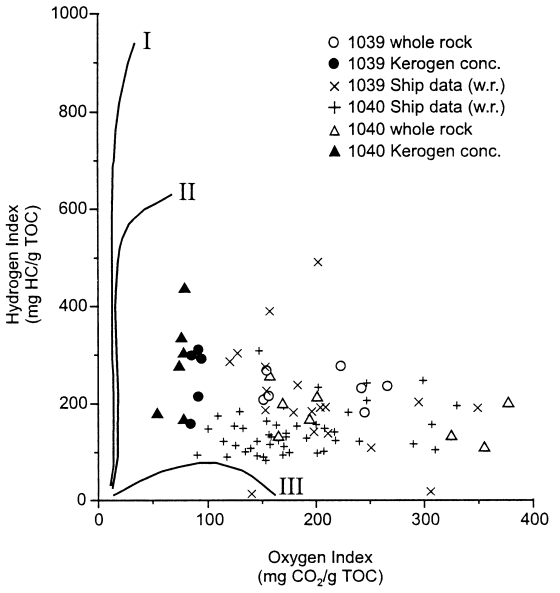

Fig. 6. HI and OI values determined on sediments (open symbols) and kerogen concentrates (solid symbols) from Sites 1039 and 1040. Measurements of ship data were made onboard JOIDES Resolution by Andreas Lückge. (Kerogen evolution paths after Espitalié et al. 1977).

and 800 mg CO_2/g TOC (values beyond 400 mg CO_2/g TOC are not plotted on Fig. 6). Such high values are not recorded in HI/OI diagrams by Espitalié et al. (1985) and Tissot and Welte (1984). The high amount of CO_2 is due to thermal decomposition of carbonates; this is a common problem if Rock-Eval pyrolysis is applied to young, carbonate-bearing marine sediments (Katz, 1983; Peters, 1986). Accordingly, OI values of kerogen concentrates are significantly lower, and vary between 84 and 94 mg CO_2/g TOC. OI values of whole rock samples and kerogen concentrates from Site 1040 show the same characteristics. OI values of whole rock samples vary between 90 and 377 mg CO_2/g TOC and those of kerogen concentrates between 54 and 79 mg CO_2/g TOC. HI values of whole rock samples range from 83 to 308 mg HC/g TOC and those of kerogen concentrates from 166 to 435 mg HC/g TOC. The HI/OI values plot between the evolution paths of Type II and Type III kerogens (Fig. 6). This can be due to either an incorporation of oxygen into Type II kerogen (Horsfield et al., 1994) or the presence of a mixture of Type II and Type III kerogens. The kerogen concentrates of Site 1040 have slightly lower OI values than those of Site 1039 which can be due to less intense oxidation at Site 1040 as a result of sulfate being the limiting factor of organic matter oxidation by bacterial sulfate reduction (see above). T_{max} values of whole rock samples and kerogen concentrates from both sites are less than 424°C thus indicating that the kerogen is immature.

Microscopic studies on kerogen concentrates and sediments revealed that the majority of the organic matter consists of brown or dark-brown unstructured organic matter. This unstructured organic matter appears as aggregates ranging in size from several micrometers up to 50 μm. The shape of these aggregates varies greatly. Unstructured organic matter can be termed amorphous organic matter (Senftle et al., 1987; Taylor et al., 1998). The content of structured macerals in samples of Site 1039 varies between 1 and 10%. The highest ratio of terrigenous organic matter occurs in a near-surface sample (1.93 mbsf). Macerals of the inertinite group contribute 5% to the organic matter. Besides inertodetrinite, fusinite can be identified from the presence of typical cell structures. Fungal remnants, sclerotinite, can be identified as well. Vitrinites are rare and contribute only 2% to the organic matter. They range in size from a few micrometers up to 25 μm. The liptinite

maceral group is mainly represented by liptodetrinites. Their diameter is usually less than 10 μm. Other liptinites range in size from 20 to 40 μm, but do not show a distinct shape. The liptinite group contributes 3% to the organic matter. With increasing depth the amount of unstructured organic matter increases. At greater depth the content of terrigenous structured macerals decreases to ~1% and the macerals show strong fragmentation.

Microscopic studies on sediments and kerogen concentrates from Site 1040 revealed that the composition of organic matter above and below the decollement differs. In the sediments of the accretionary prism an enhanced contribution of terrigenous organic matter is obvious. The portion of the unstructured organic matter varies between 92% and 95%. Below the decollement, it increases to 97–99%. Reflectance measurements on autochthonous vitrinites of both sites revealed an average value of 0.26% R_r which indicates a very low maturity.

High contents of unstructured organic matter are typical for upwelling areas, i.e. areas of high primary productivity (Littke and Sachsenhofer, 1994). Also other deep marine sediments rich in organic matter are characterized by a predominance of unstructured organic matter (e.g. Thurow et al., 1992). Sediments underlying coastal upwelling areas usually contain more than 2% TOC. An upwelling regime does not exist off Costa Rica and the organic carbon contents of the studied sediments are less than 1.6%. High contents of unstructured organic matter can be explained here by enhanced bioproductivity (as described above). The expected dominance of terrigenous over marine particles in trench-slope transition zones (Littke and Sachsenhofer, 1994) cannot be found, because the Middle America Trench off Costa Rica is nearly devoid of turbidites (Shipley et al., 1992). This fact provides further evidence that the contribution of terrigenous organic matter transported by wind is not very important; otherwise a higher percentage could be expected here. Only at the slope a slightly higher portion of terrigenous and recycled particles contributes to the organic matter.

5.4. Distribution of biomarkers

5.4.1. n-Alkanes

The aliphatic hydrocarbon fractions of the studied samples are dominated by *n*-alkanes with chain lengths between C_{13} and C_{42}. At Site 1039, contents of the summed C_{13}–C_{42} *n*-alkanes vary between 100 and 300 μg/g TOC with the exception of two samples at shallow depths which show significantly elevated contents of *n*-alkanes (Fig. 7). No clear depth related trend for the *n*-alkane contents is observed at Site 1039. At Site 1040, contents of *n*-alkanes in sediments below the decollement are in the same order as at Site 1039 while higher contents of *n*-alkanes are observed in the accretionary prism showing a generally decreasing trend with increasing depth. Below the decollement the distributions of *n*-alkanes at Site 1040 are similar to those observed for Site 1039 (Fig. 8) but the CPI_{HC} curve is more compressed because of the greater compaction of the sediments at Site 1040 (Fig. 7).

The bar charts in Fig. 8 depict the relative distribution of *n*-alkanes and the isoprenoidal hydrocarbons pristane and phytane in selected samples from Sites 1039 and 1040. In most of the samples, a bimodal distribution of *n*-alkanes is observed. Long-chain *n*-alkanes with strong odd-over-even predominance (OEP) maximising at C_{29}, C_{31} and C_{33} can be attributed to cuticular waxes of higher plants (Kolattukudy, 1980) and hence to the contribution of organic matter derived from terrestrial plants. The second maximum of *n*-alkanes is observed at shorter chain lengths around C_{18}, C_{20} or C_{22}. In contrast to the above mentioned long-chain *n*-alkanes these distributions are often related to organic matter of higher maturity (Peters and Moldowan, 1993). Therefore, the presence of these shorter-chain *n*-alkanes could indicate impregnation of the sediments with migrated bitumen deriving from organic matter of higher thermal maturity. The systematically increasing values of CPI_{HC} below 100 mbsf at Site 1039 and 450 mbsf at Site 1040 (Fig. 7) might be regarded as additional evidence for an increasing contribution of bitumen migrated from underlying sediments.

However, these considerations do not readily explain the even-over-odd predominance (EOP) observed for some of the samples (Fig. 7). The EOP is most pronounced in the shallowest sample from Site 1039 where the shorter chain *n*-alkanes are clearly dominating but can also be recognized in other samples, e.g. at Site 1040 at a depth of 462 mbsf (Fig. 7). EOP is characteristic for bitumens and crude oils from carbonate and hypersaline environments (Peters and Moldowan, 1993). Interestingly, at both sites higher CPI_{HC} values (Fig. 7) roughly coincide with higher contents of $CaCO_3$, although with some scatter (Figs. 2 and 3). Furthermore, it must be assumed that EOP is associated with reducing conditions under which even-numbered *n*-alkanes may be formed due to the reduction of the corresponding even-numbered fatty acids and/or alcohols. It is well documented that a broad range of marine microalgae contain significant amounts of (unsaturated) C_{18}–C_{24} *n*-fatty acids (e.g. Volkman et al., 1989) and may be the source of these compounds in marine sediments (e.g. Budge and Parrish, 1998). Reduction of such lipids during early diagenesis should result in *n*-alkane patterns similiar to those observed for the shallow samples from Site 1039.

From TOC/S ratios below 2.8 for most of the samples oxygen-depleted depositional conditions are very likely (see above). It is noteworthy that — with the exception of one sample — pristane / phytane ratios are generally

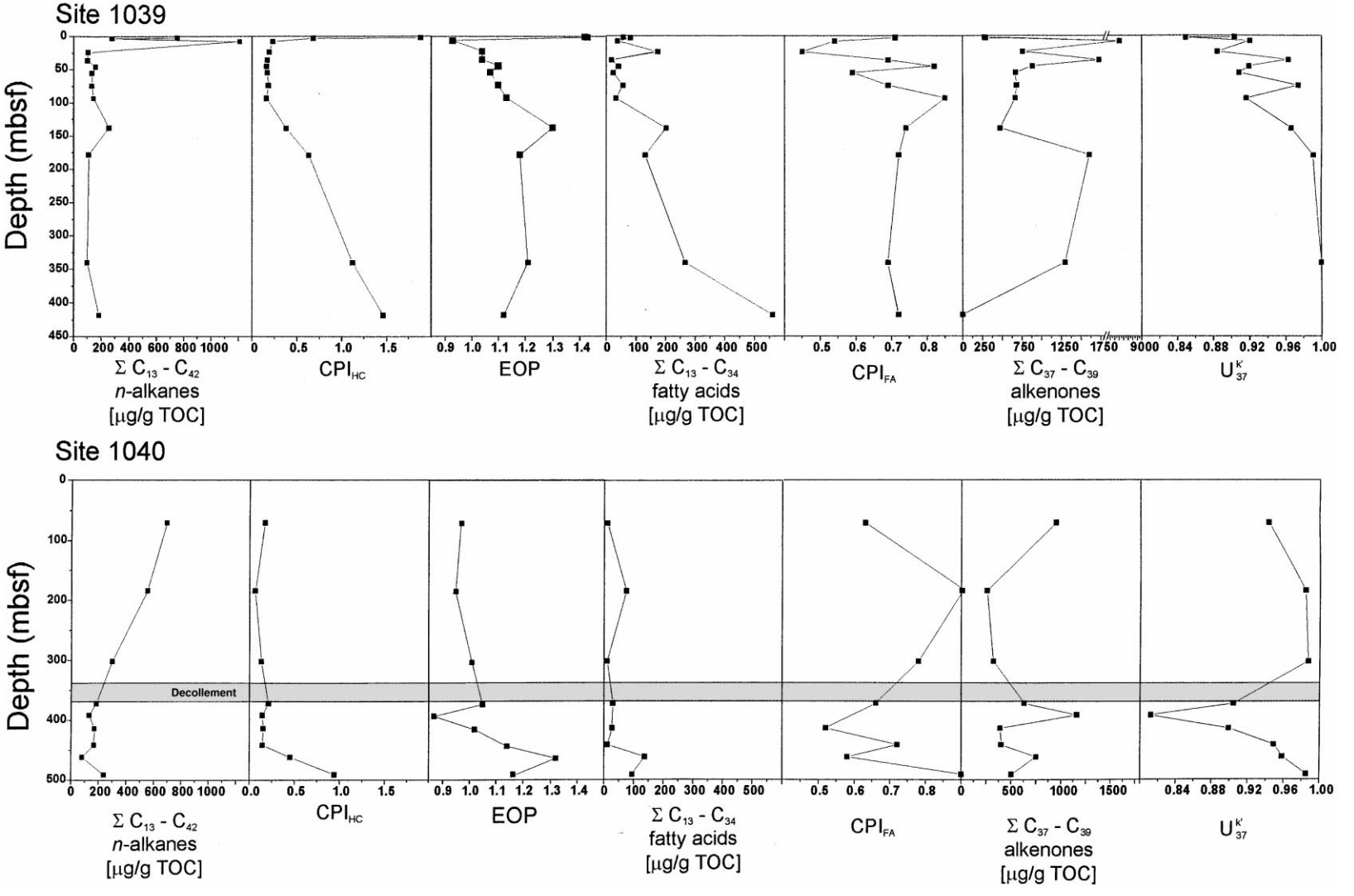

Fig. 7. Summed *n*-alkane-, fatty acid- and alkenone concentrations of Sites 1039 and 1040 and the calculated CPI_{HC}, *EOP*, CPI_{FA} and U^{k}_{37} values of both sites.

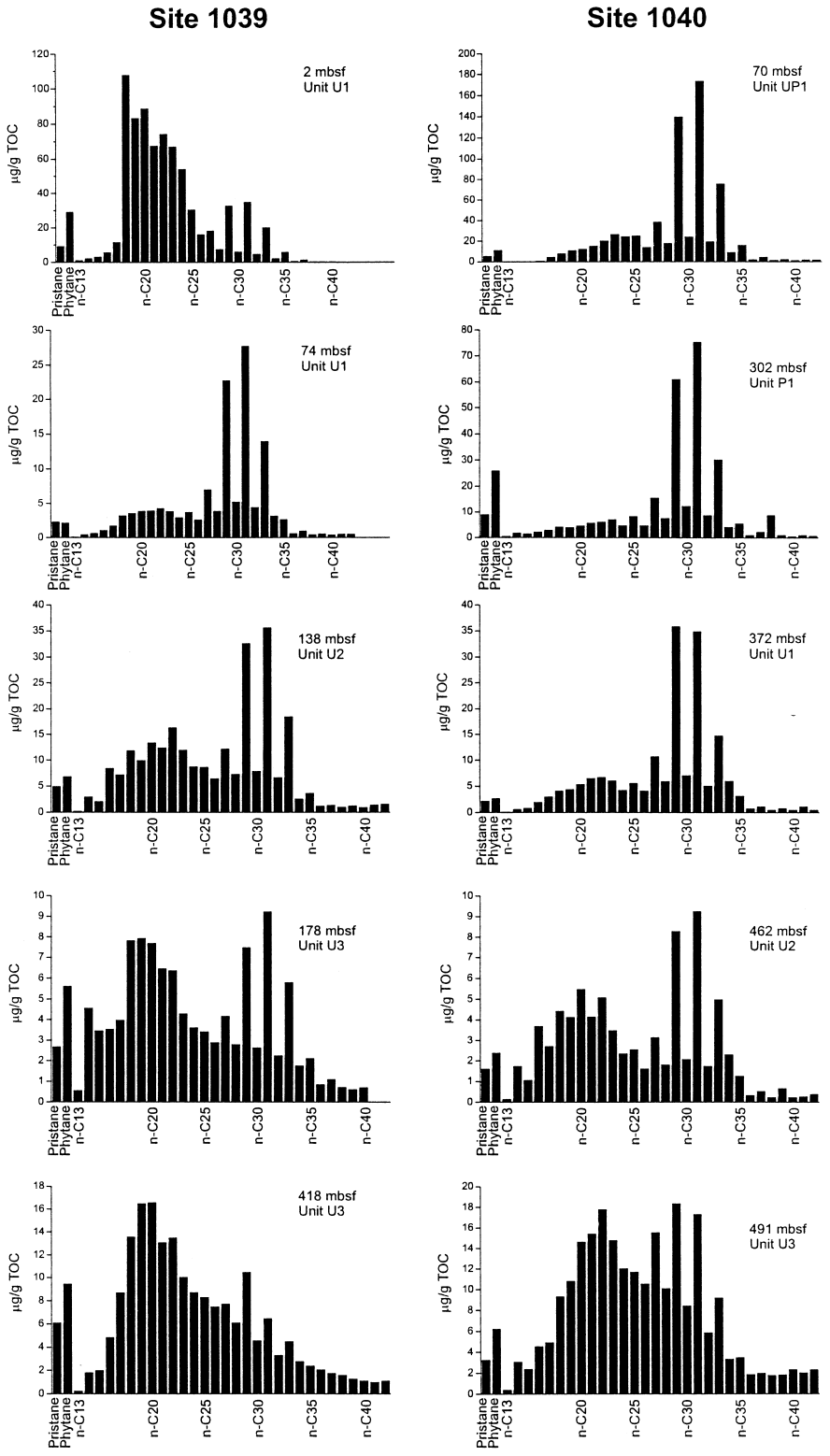

Fig. 8. Distribution of *n*-alkanes and pristane and phytane in samples from Site 1039 (left) and Site 1040 (right).

below 1 also pointing to a reducing depositional environment. We, therefore, conclude that the presence of shorter chain *n*-alkanes in these sediments indeed is due to the contribution of diagenetically altered algal lipids rather than impregnation with migrated bitumen. This implies that the observed variations of CPI_{HC} might indicate some variations of the redox conditions. From the *n*-alkane patterns observed at Site 1039 it turns out that a major shift to less reducing conditions must have occurred during the Late Pliocene/Early Pleistocene. The much higher CPI_{HC} values in the two shallowest samples from Site 1039 provide evidence for another shift towards more reducing conditions during the Late Pleistocene/Holocene. The low relative amounts of C_{18}–C_{24} *n*-alkanes throughout most of the Pleistocene would then point to conditions under which diagenetic pathways other than reduction are the major control on the sedimentary fate of the biogenic lipids.

From these considerations it turns out that the use of *n*-alkanes as source specific biomarkers for assignment of terrestrial versus marine organic matter is difficult for the investigated profiles due to the influence of changing diagenetic processes. Some useful information may nevertheless be obtained with respect to the relative importance of terrigenous contributions from land plants. In the sample from 7.93 mbsf at Site 1039 the concentration of the C_{27}, C_{31} and C_{33} *n*-alkanes is one order of magnitude higher than in all other samples from Site 1039 suggesting a strong predominance of terrigenous organic matter. The significantly elevated yields of long-chain *n*-alkanes in the sediments of the accretionary prism of Site 1040 also indicate a contribution of terrigenous organic matter which probably is significantly higher than in the subducted sediments.

5.4.2. Fatty acids

Contents of *n*-fatty acids in sediments from Sites 1039 and 1040 are generally low (Fig. 7). At Site 1039 they show systematically increasing yields with increasing depth. The maximum content of approximately 500 μg/g TOC for the summed C_{13}–C_{34} *n*-fatty acids was determined for the deepest sample. The contents of *n*-fatty acids at Site 1040 are even lower. However, a principal increase of yields with increasing depth below the decollement is in principal agreement with the data obtained for Site 1039. The low yields of fatty acids may be explained to some extent by losses due to diagenetic transformation processes and in particular to reduction yielding the corresponding *n*-alkanes as discussed in the previous section.

In general, *n*-fatty acid distributions are dominated by palmitic acid (C_{16}) and stearic acid (C_{18}) in most samples. At Site 1039 only one sample (24 mbsf) is dominated by long-chain fatty acids from the cuticular waxes of higher plants maximizing at hexacosanoic acid (C_{26}). Samples from Site 1040 are also dominated by short-chain fatty acids (C_{13}–C_{18}), especially palmitic and stearic acid. Higher amounts of long-chain fatty acids (C_{22}–C_{32}) are present in the sediments of the accretionary prism at shallow depth (< 80 mbsf) and immediately below the decollement.

For Site 1039 CPI_{FA} values are almost generally above 0.5 (Fig. 7). This predominance of short-chain fatty acids indicates that the organic matter is mainly of marine origin which is in agreement with the results of the microscopic investigations. It appears that the fatty acids might be a better indicator of terrigenous versus marine organic matter input than the *n*-alkanes. Nevertheless, qualitative interpretations derived from *n*-alkanes and fatty acids are in principal agreement. A significantly higher relative contribution of terrigenous organic matter to sediments between 6 and 100 mbsf at Site 1039 and in the accretionary prism of Site 1040 in comparison to other parts of the profiles is inferred from both the *n*-alkane and the *n*-fatty acid distributions. In the uppermost 100 m of the profile from Site 1039 CPI_{FA} shows strong fluctuations in contrast to the more or less negligible fluctuations of CPI_{HC} probably indicating significant variations of terrigenous versus marine organic matter supply during the Quaternary.

5.4.3. Alkenones

Long-chain di-, tri- and tetraunsaturated methyl- and ethylketones (long-chain alkenones) are produced by Haptophyceae, i.e. *Emiliania huxleyi* and *Gephyrocapsa oceanica* (Marlowe et al., 1984; Volkman et al., 1995). These compounds are now well established as a tool for the determination of paleo sea surface temperatures (SSTs) (Brassell, 1993).

Summed alkenone contents in sediment samples from both sites vary between 250 and 2000 μg/g TOC with the exception of one sample from Site 1039 (7.93 mbsf) with a total alkenone content as high as 8000 μg/g TOC (Fig. 7). No systematic depth related trend of alkenone contents is observed. In particular, the alkenone content normalized to TOC does not decrease with increasing depth indicating that the alkenones are not lost at higher rates than other fractions of the biogenic organic matter during diagenesis.

U^{k}_{37} values vary between 0.94 and 0.97 in the accretionary prism (Fig. 9) of Site 1040 corresponding to SSTs between 27 and 28°C based on the calibration of Müller et al. (1998). This is in principal agreement with present-day SSTs off Costa Rica being above 25°C throughout the year. Below the decollement U^{k}_{37} values increase with increasing depth from 0.81 to 0.98. This would indicate that the SSTs during the Miocene and Pliocene decreased from 28 to 23.5°C. U^{k}_{37} values at Site 1039 show a similar increasing trend with increasing depth as the subducted sediments from Site 1040. However, significant fluctuations of the U^{k}_{37} values are

observed during the Quaternary at this site which are not recognized at Site 1040 most probably due to the limited number of analyzed samples. A possible explanation for this variability is a relationship with glacial/interglacial changes. Local minima of U^{k}_{37}at 45.8 and 55.3 mbsf and local maxima of U^{k}_{37} at 36.3 and 74.3 mbsf correspond to glacial and interglacial periods, respectively, based on oxygen isotopes (Shackleton and Opdyke, 1976). However, a much higher resolution would be necessary to confirm this assumption.

U^{k}_{37} data obtained for Sites 1039 and 1040 are in principal agreement with previous reports on alkenones in the equatorial Pacific. A study in the central equatorial Pacific (0°57′N, 138°57′W) revealed small variations of less then 3°C for SSTs fluctuating between 24.5 and 27.5°C over the past 250 ka (Lyle et al., 1992). Even smaller variations between 27 and 28°C were obtained for a 20 ka record from the western equatorial Pacific (3°32′N, 141°52′E) (Ohkouchi et al., 1994). Stronger SST variations between 19 and 28°C were determined in a high resolution study of ODP Site 846 (300 km south of Galapagos, 3°06′S, 90°49′W) covering the past 1.3 Myr (Emeis et al., 1995). The lower SSTs at this site were explained by the advection of cold water into the South Equatorial Current which is merged by the Peru Current. Consequently, low SSTs ranging from 18 to 23.5°C were obtained for Peru margin surface sediments (different locations between 11 and 15°S) (McCaffrey et al., 1990).

In general, not much attention has been paid to the occurrence of long-chain alkenones in relatively old sediments. U^{k}_{37} values determined for sediments from the New Jersey continental margin correspond to SSTs varying from 17°C to 28°C during the last 45 Ma without any significant depth trend (van der Smissen and Rullkötter, 1996). In Cretaceous black shales from the Blake-Bahama Basin which are of Cenomanian and mid-Albian age (95 and 105 Ma, respectively) only alkadienones were identified (Farrimond et al., 1986). An increasing trend of U^{k}_{37} values with increasing age has been observed for Neogene sediments from the Southern Canary Channel (Wilkes et al., 1997). A prerequisite for the use of long-chain alkenones as temperature indicators in older sediments is that the calibrations are valid over long geological time periods. It may not be overlooked that *Emiliania huxleyi* the main producer of the alkenones in the open oceans first appeared in the fossil record in the late Quaternary some 265 kyr ago (Thierstein et al., 1977). Long-chain alkenones found in older sediments such as investigated in this study, therefore, might be produced by extinct species and hence possible temperature relationships are unknown. Finally, it cannot be excluded that alkatrienones are lost at higher rates than alkadienones during diagenesis (e.g. Gong and Hollander, 1999) which would also be a possible explanation for the general increase of U^{k}_{37} values with increasing depth observed at Sites 1039 and 1040. More studies on the occurrence and distribution of long-chain alkenones throughout the Cenozoic are necessary to adequately judge their possible usefulness as a paleoenvironmental tools beyond the Quaternary.

6. Conclusions

The organic matter in the sediments is mainly of marine origin. Microscopic studies revealed that most of the kerogen consists of unstructured organic matter. Macerals, derived from terrigenous sources (vitrinite, inertinite, some liptinites), contribute a maximum of 10% to the organic matter. Sulfur is mainly fixed as pyrite. The remaining sulfur is fixed in inorganic sulfur-containing compounds and incorporated in the kerogen. Sulfur/organic carbon ratios are generally high indicating a significant loss of organic matter in the sediments due to sulfate reduction. The *n*-alkane distributions are characterized by an even-over-odd predominance in most of the samples which is due to a high decay of marine derived organic matter under reducing conditions. In some of the shallower samples, long-chain *n*-alkanes indicate the presence of terrigenous organic matter, in particular down to a depth of about 200 mbsf at Site 1039. Fatty acid distributions show similar trends, also demonstrating that the organic matter is mainly of marine origin. Organic carbon contents in Miocene sediments of less than 0.2%, caused by low primary productivity and dilution with carbonate, result in a low degree of sulfate reduction in the Miocene at this site. The increase in primary productivity in the Pliocene and Pleistocene and the enhanced supply of terrigenous organic matter in the Pleistocene can be related to the drift of the Cocos plate to a near-shore position. Constantly high $U^{k'}_{37}$ values in the Miocene and Pliocene indicate sea-surface temperatures of more than 27°C. The larger variations in $U^{k'}_{37}$ values during the Pleistocene are probably the response to glacial/interglacial changes. Subduction had little influence on the composition of organic matter because temperatures are still low. With prograding subduction the organic matter will be altered significantly.

Acknowledgements

The authors have benefited from a thorough review of the manuscript by Dr. J. Volkman and Dr. F. Baudin. The authors thank E. Biermanns, W. Laumer, F. Leistner, R. Mildenberger, A. Richter and H. Willsch for technical support. Financial support by the Deutsche Forschungsgemeinschaft (grant no. Li 618/2) is gratefully acknowledged as well as support by the ODP community

References

Berger, W.H., Smetacek, V.S., Wefer, G., 1989. Ocean productivity and paleoproductivity — an overview. In: Berger, W.H., Smetacek, V.S., Wefer, G. (Eds.), Productivity of the Ocean: Present and Past.. John Wiley and Sons, Chichester, pp. 1–34.

Berner, R.A., 1983. Sedimentary pyrite formation: an update. Geochimica et Cosmochimica Acta 48, 605–615.

Berner, R.A., Raiswell, R., 1983. Burial of organic carbon and pyrite sulfur in sediments over Phanerozoic time: a new theory. Geochimica et Cosmochimica Acta 47, 855–862.

Brassell, S.C., 1993. Applications of biomarkers for delineating marine paleoclimatic fluctuations during the Pleistocene. In: Engel, M.H., Macko, S.A. (Eds.), Organic Geochemistry. Plenum Press, New York, pp. 699–738.

Brassell, S.C., Eglinton, G., Marlowe, I.T., Pflaumann, U., Sarnthein, M., 1986. Molecular stratigraphy: a new tool for climatic assessment. Nature 320, 129–133.

Budge, S.M., Parrish, C.C., 1998. Lipid biogeochemistry of plankton, settling matter and sediments in Trinity Bay, Newfoundland. II. Fatty acids. Organic Geochemistry 29, 1547–1559.

Calvert, S.E., Pedersen, T.F., 1992. Organic carbon accumulation and preservation in marine sediments: How important is anoxia?. In: Whelan, J.K., Farrington, J.W. (Eds.), Organic Matter, Productivity, Accumulation and Preservation, in Recent and Ancient Sediments. Columbia Univ. Press, New York, pp. 231–263.

Canfield, D.E., 1989. Sulfate reduction and oxic respiration in marine sediments: implications for organic carbon preservation in euxinic environments. Deep-Sea Research 36, 121–138.

Chester, R., 1990. Marine Geochemistry, Unwin Hyman Ltd, London.

Durand, B., Nicaise, G., 1980. Procedures for kerogen isolation. In: Durand, B. (Ed.), Kerogen. Insoluble Organic Matter From Sedimentary Rocks. Edition Technip, Paris, pp. 35–53.

Emeis, K.-C., Doose, H., Mix, A., Schulz-Bull, D., 1995. Alkenone sea-surface temperatures and carbon burial at site 846 (Eastern Equatorial Pacific Ocean): the last 1.3 M.Y. In: Pisias, N.G., Mayer, L.A., Janecek, T.R., Palmer-Julson, A., van Andel, T.H. (Eds.), Proc. ODP, Sci. Results, 138. College Station. (Ocean Drilling Program), TX, pp. 605–613.

Espitalié, J., Deroo, G., Marquis, F., 1985. La pyrolyse Rock-Eval et ses applications. Institut Francais du Pétrole 40, 536–579.

Espitalié, J., Laporte, J.L., Madec, M., Marquis, F., Leplat, P., Paulet, J., Boutefeu, A., 1977. Méthode rapide de charactérization des roches mères de leur potentiel pétrolier et de leur degré d'evolution. Revue de L'Institut Francais du Pétrole 32, 23–42.

Farrimond, P., Eglinton, G., Brassell, S.C., 1986. Alkenones in Cretaceous black shales, Blake-Bahama Basin, western North Atlantic. Organic Geochemistry 10, 897–903.

Frisch, W., Loeschke, J., 1993. Plattentektonik. Wissenschaftliche Buchgesellschaft, Darmstadt.

Gong, C., Hollander, D.J., 1999. Evidence for differential degradation of alkenones under contrasting bottom water oxygen conditions: implications for paleotemperature reconstruction. Geochimica et Cosmochimica Acta 63, 405–411.

Hinz, K., Von Huene, R., Ranero, C.R., 1996. Tectonic structure of the convergent Pacific margin offshore Costa Rica from multichannel seismic reflection data. Tectonics 15, 54–66.

Horsfield, B., Curry, D.J., Bohacs, K., Littke, R., Rullkötter, J., Schenk, H.J. et al., 1994. Organic geochemistry of freshwater and alkaline lacustrine sediments in the Green River Formation of the Washakie Basin, Wyoming, USA. Organic Geochemistry 22, 415–440.

Katz, B.J., 1983. Limitations of Rock-Eval pyrolysis for typing organic matter. Organic Geochemistry 4, 195–199.

Kimura, G., Silver, E., Blum, P. et al., 1997. Proc. ODP, Init. Repts., 170: College Station, TX (Ocean Drilling Program).

Koblents-Mishke, O.I., Volkovinsky, V.V., Kabanova, Y.G., 1970. Plankton primary production of the World Ocean. In: Wooster, W. (Ed.), Scientific Exploration of the South Pacific. Nat. Acad. Sci, Washington, pp. 183–193.

Kolattukudy, P.E., 1980. Cutin, suberin and waxes. In: Stumpf, P.K. (Ed.), The Biochemistry of Plants, vol. 4, Lipids: Structure and Function. Academic Press, New York. pp, 571–, pp. 645–.

Langseth, M.G., Silver, E.A., 1996. The Nicoya convergent margin — a region of exceptionally low heat flow. Geophysical Research Letters 23, 891–894.

Littke, R., Baker, D.R., Rullkötter, J., 1997a. Deposition of petroleum source rocks. In: Welte, D.H., Horsfield, B., Baker, D.R. (Eds.), Petroleum and Basin Evolution . Springer, Heidelberg, pp. 271–333.

Littke, R., Lückge, A., Welte, D.H., 1997b. Quantification of organic matter degradation by microbial sulphate reduction for Quaternary sediments from the Northern Arabian Sea. Naturwissenschaften 84, 312–315.

Littke, R., Lückge, A., Wilkes, H., 1998. Organic matter in Neogene sediments of the southern Canary Channel, Canary Islands (Sites 955 and 956). In: Weaver, P.P.E., Schmincke, H.-U., Firth, J.V., Duffield, W. (Eds.), Proceedings of the Ocean Drilling Program, Scientific Results 157. College Station, TX, pp. 361–372.

Littke, R., Sachsenhofer, R.F., 1994. Organic petrology of deep sea sediments: a compilation of results from the Ocean Drilling Program and the Deep Sea Drilling Project. Energy and Fuels 8, 1498–1512.

Lyle, M.W., Prahl, F.G., Sparrow, M.A., 1992. Upwelling and productivity changes inferred from a temperature record in the central equatorial Pacific. Nature 355, 812–815.

McCaffrey, M.A., Farrington, J.W., Repeta, D.J., 1990. The organic geochemistry of Peru margin surface sediments: I. A comparison of the C37 alkenone and historical El Ni records. Geochimica et Cosmochimica Acta 54, 1671–1682.

Marlowe, I.T., Grenn, J.C., Neal, A.C., Brassell, S.C., Eglinton, G., Course, P.A., 1984. Long chain alkenones in the Prymnesiophyceae-Distributions of alkenones and their taxonomic significance. British Journal of Phycology 19, 203–216.

Müller, P.J., Kirst, G., Ruhland, G., Storch, E., Rosell-Melé, A., 1998. Calibration of the alkenone paleotemperature index U^{k}_{37} based on core-tops from the eastern South Atlantic and the global ocean (60°N–60°S). Geochimica et Cosmochimica Acta 62, 1757–1772.

Ohkouchi, N., Kawamura, K., Nakamura, T., Taira, A., 1994. Small changes in the sea surface temperature during the last 20,000 years: molecular evidence from the western tropical Pacific. Geophysical Research Letters 21, 2207–2210.

Pedersen, T.F., Calvert, S.E., 1990. Anoxia vs. productivity: what controls the formation of organic-carbon-rich sediments and sedimentary rocks AAPG Bulletin 74, 454–466.

Peters, K.E., 1986. Guidelines for evaluating petroleum source rock using programmed pyrolysis AAPG Bulletin 70, 318–329.

Peters, K.E., Moldowan, J.M., 1993. The Biomarker Guide, Prentice Hall, Englewood Cliffs.

Radke, M., Willsch, H., Welte, D.H., 1978. Removal of soluble organic matter from rock samples with a flow-through extraction cell. Analytical Chemistry 50, 663–665.

Senftle, J.T., Brown, J.H., Larter, S.R., 1987. Refinement of organic petrographic methods for kerogen characterization. International Journal of Coal Geology 7, 105–117.

Shackleton, N.J., Opdyke, N.D., 1976. Oxygen-isotope and paleomagnetic stratigraphy of Pacific Core V28-239, late Pliocene to latest Pleistocene. Memoir — Geological Society of America 145, 449–464.

Shipley, T.H., McIntosh, K.D., Silver, E.A., 1992. Three-dimensional seismic imaging of the Costa Rica accretionary prism: Structural Diversity in a small volume of the lower slope. Journal of Geophysical Research 97, 4439–4459.

Sinninghe Damsté, J.S., Eglinton, T.I., De Leeuw, J.W., Schenck, P.A., 1989. Organic sulphur in macromolecular sedimentary organic matter: I. Structure and origin of sulphur-containing moieties in kerogen, asphaltenes and coal as revealed by flash pyrolysis. Geochimica et Cosmochimica Acta 53, 873–889.

Stein, R. 1986. Surface-water paleo-productivity as inferred from sediments deposited in oxic and anoxic deep-water environments of the Mesozoic Atlanic Oceanic. In Degens, E. T. (Ed.), Mitteilungen des Geologisch-Paläontologischen Instituts der Universität Hamburg Vol. 60. pp. 55–70.

Stein, R., 1991. Accumulation of Organic Carbon in Marine Sediments, Springer, Heidelberg.

Taylor, G.H., Teichmüller, M., Davis, A., Diessel, C.F.K., Littke, R., Robert, P., 1998. Organic Petrology, Borntraeger, Berlin.

Thierstein, H.R., Geitsenauer, K.R., Molfino, B., Shackleton, N.J., 1977. Global synchroneity of late Quaternary coccolith datum levels: validation by oxygen isotopes. Geology 5, 400–404.

Thurow, J., Brumsack, H.-J., Rullkötter, J., Littke, R., Meyers, P., 1992. The Cenomanian/Turonian boundary event in the Indian Ocean — a key to understand the global picture. Geophysical Monograph 70, 253–273.

Tissot, B.P., Welte, D.H., 1984. Petroleum Formation and Occurrence, Springer, Berlin.

Van der Smissen, J.H., Rullkötter, J., 1996. Organofacies variations in sediments from the continental slope and rise of the New Jersey continental margin (Sites 903 and 905). In: Mountain, G.S., Miller, K.G., Blum, P., Poag, C.W., Twichell, D.C. (Eds.), Proceedings of the Ocean Drilling Program, Scientific Results, Vol. 150. (Ocean Drilling Program), College Station, TX, pp. 329–344.

Volkman, J.K., Barrett, S.M., Blackburn, S.I., Sikes, E.L., 1995. Alkenones in Gephyrocapsa oceanica: implications for studies of paleoclimate. Geochimica et Cosmochimica Acta 59, 513–520.

Volkman, J.K., Jeffrey, S.W., Nichols, P.D., Rogers, G.I., Garland, C.D., 1989. Fatty acid and lipid composition of 10 species of microalgae used in mariculture. Journal of Experimental Marine Biology and Ecology 128, 219–240.

Von Huene, R., Aubouin, J., 1985. Site 565, Inital Reports of the Deep Sea Drilling Project, 84: Washington (US Govt. Printing Office).

Wilkes, H., Littke, R., Lückge, A., Willsch, H., 1997. Long-chain alkenones in Neogene sediments of the Southern Canary Channel, Canary Islands (ODP Site 955). In: Abstracts of the 18th International Meeting on Organic Geochemistry, 22–26. September 1997, Maastricht, The Netherlands, pp. 617–618.

Willsch, H., Clegg, H., Horsfield, B., Radke, M., Wilkes, H., 1997. Liquid chromatographic separation of sediment, rock, and coal extracts and crude oil into compound classes. Analytical Chemistry 69, 4203–4209.